Journal of Geophysical Research: Space Physics

RESEARCH ARTICLE
10.1002/2017JA024941

Influence of the IMF Cone Angle on Invariant Latitudes of Polar Region Footprints of FACs in the Magnetotail: Cluster Observation

Z. W. Cheng[1], J. K. Shi[1,2], J. C. Zhang[3], K. Torkar[4], L. M. Kistler[3], M. Dunlop[5], C. Carr[6], H. Rème[7], I. Dandouras[7], and A. Fazakerley[8]

[1]State Key Laboratory of Space Weather, NSSC/CAS, Beijing, China, [2]Schools of Astronomy and Space Science, University of Chinese Academy of Sciences, Beijing, China, [3]Space Science Center, University of New Hampshire, Durham, NH, USA, [4]Space Research Institute, Austrian Academy of Sciences, Graz, Austria, [5]Rutherford Appleton Laboratory, Chilton, Didcot, UK, [6]Blackett Laboratory, Space and Atmospheric Physics Group, Imperial College, London, UK, [7]University of Toulouse, UPS, IRAP, and CNRS, Toulouse, France, [8]MSSL, University College London, Dorking, UK

Key Points:
- Only the equatorward boundary of polar region footprints of FACs in the magnetotail lowers with increasing IMF cone angle
- The footprints of FACs (with large density) are located at ILAT < 71° and mainly correspond to large IMF cone angles (theta > 60°)
- The relationship between polar region footprints of FACs in the PSBL and the IMF cone angle is determined for the first time

Correspondence to:
Z. W. Cheng,
zwcheng@spaceweather.ac.cn

Citation:
Cheng, Z. W., Shi, J. K., Zhang, J. C., Torkar, K., Kistler, L. M., Dunlop, M., et al. (2018). Influence of the IMF cone angle on invariant latitudes of polar region footprints of FACs in the magnetotail: Cluster observation. *Journal of Geophysical Research: Space Physics*, *123*, 2588–2597. https://doi.org/10.1002/2017JA024941

Received 3 NOV 2017
Accepted 8 MAR 2018
Accepted article online 13 MAR 2018
Published online 6 APR 2018

Abstract The influence of the interplanetary magnetic field (IMF) cone angle θ (the angle between the IMF direction and the Sun-Earth line) on the invariant latitudes of the footprints of the field-aligned currents (FACs) in the magnetotail has been investigated. We performed a statistical study of 542 FAC cases observed by the four Cluster spacecraft in the Northern Hemisphere. The results show that there are almost no FACs when the IMF cone angle is less than 10°, and there are indications of the FACs in the plasma sheet boundary layers being weak under the radial IMF conditions. The footprints of the large FAC (>10 nA/m^2) cases are within invariant latitudes <71° and mainly within IMF cone angles $\theta > 60°$, which implies that the footprints of the large FACs mainly expand equatorward with large IMF cone angle. The equatorward boundary of the FAC footprints in the polar region decreases with increasing IMF cone angle (and has a better correlation for northward IMF), which shows that the IMF cone angle plays an important controlling role in FAC distributions in the magnetosphere-ionosphere coupling system. There is almost no correlation between the poleward boundary and the IMF cone angle for both northward and southward IMF. This is because the poleward boundary movement is limited by an enhanced lobe magnetic flux. This is the first time a correlation between FAC footprints in the polar region and IMF cone angles has been determined.

1. Introduction

Field-aligned currents (FACs) were detected by satellites for the first time in the 1960s (Cummings & Dessler, 1967; Zmuda et al., 1966), and they have been observed at both low (Iijima & Potemra, 1978) and high (Frank, 1981) altitudes in different regions in geospace. The large-scale (reaching from the magnetotail to the ionosphere) FACs are involved in many important physical processes, including field-aligned particle acceleration (Choy et al., 1971; Morooka et al., 2004; Shi et al., 2014), magnetic reconnection in the magnetotail (Hones, 1979; Ma & Otto, 2013; Scholer & Otto, 1991), development of the substorm current wedge (Hesse & Birn, 1991; Pytte et al., 1976), and auroral activity (Elphic et al., 1998; Xiong et al., 2014).

In solar wind-magnetosphere-ionosphere interactions, the large-scale FAC plays a crucial role in transferring the solar wind momentum and energy to magnetosphere and ionosphere. The interplanetary parameters directly affect the energy transfer process and the associated FACs. In the polar region, the dependence of FAC characteristics on the interplanetary magnetic field (IMF) components has been studied (Yamauchi & Araki, 1989; Masakazu & Sofko, 2009). Iijima and Shibaji (1987) reported that the variation of IMF B_y can lead to the dawn-dusk asymmetry of FACs. Taguchi et al. (1992) found that the FAC intensity is controlled by the IMF and enhances with the IMF $|B_y|$. Some other authors reported that the IMF B_z is also an important control factor (Gjerloev et al., 2011; Juusola et al., 2009). From above authors' studies, we can conclude that the FACs are affected by more than one IMF component. Li et al. (2011) showed that the IMF clock angle is a major factor to control the FACs associated with Joule heating.

In the magnetosphere, the importance of the IMF cone angle is not controversial because it is closely related to many important physical phenomena. Some studies show that the IMF cone angle affects geomagnetic pulsations (Pc2–5 pulsations) (Takahashi et al., 1984). Kavosi and Raeder (2015) found that the occurrence rate of Kelvin-Helmholtz waves in the magnetopause increases with the IMF cone angle. Also, the IMF

cone angle can control the efficiency of reconnection at the subsolar point (Scurry et al., 1994). Some authors have suggested that the IMF cone angle can even influence the magnetopause location (Dušík et al., 2010). In the magnetotail, both the IMF cone angle and clock angle are important factors and have great influence on the FACs. Cheng et al. (2013) found that the FAC occurrence in the magnetotail increases monotonically with the IMF cone angle. The FAC is a large-scale phenomenon in the magnetosphere-ionosphere system. The FACs in the plasma sheet boundary layers (PSBLs) are connected with those in the polar region through the magnetic field lines (Wild et al., 2004), and they are important for the energy flows in the solar wind-magnetosphere-ionosphere system. How the solar wind affects the large-scale FACs from the magnetotail to the polar region is still an open question. Also, there is no study on the relationship between the IMF cone angle and the polar region footprints of the FACs in the PSBLs in the magnetotail.

This study is focused on the influence of the IMF cone angle on the projection locations of the FACs observed by Cluster in the northern PSBL in the magnetotail. The results show that the IMF cone angle has a controlling role on the projection location of the FACs in the PSBLs in the magnetotail.

2. Data and Method

In this study, the magnetic field data from the Fluxgate Magnetometer (Balogh et al., 1997) on board the Cluster spacecraft were used to calculate the current density. The ion and electron data, respectively, were taken by the Cluster Ion Spectrometry (Rème et al., 2001) and the Plasma Electron And Current Experiment (Johnstone et al., 1997) instruments on board the Cluster spacecraft. The corresponding IMF, the auroral electrojet (AE) index, and the disturbance storm time (D_{st}) index were obtained from the OMNI database. The apogee of the four Cluster spacecraft is about 19.6 Earth radii (R_E), and the orbital period is about 57 hr. In 2001 (2004), the interspacecraft distance of Cluster in the magnetotail was ~2,000 km (~1,000 km). According to the period and variations of its orbit, there were about 60 days with northern PSBL crossings each year. During these crossings, the interspacecraft distances were suitable for calculating current density by the "curlometer" method (Dunlop et al., 1988).

In this study, FAC cases with densities larger than 3 pT/km, that is, 2.38 nA/m^2 (1 nA/m^2 = 1.26 pT/km), have been selected. This ensured that the background noise and the errors resulting from the current calculation are low (Shi et al., 2010). The minimum interval between two neighboring FAC cases has been set to 5 min. If there were two or more FACs densities over 3 pT/km within 5 min, the largest one was selected as a FAC case. The current in units of pT/km has been obtained directly from the calculation with the "curlometer" technique. Positive densities denote an earthward FAC.

We used plasma $ß$ to identify the plasma sheet (PS), PSBL and the lobe region. In the PSBL, it satisfies $0.01 \leq ß \leq 1$, while $ß < 0.01$ in the lobe region and $ß > 1$ in the PS (Ueno et al., 2002). The IMF cone angle "θ" is defined as follows:

$$\theta = \cos^{-1}(\mathrm{IMF}|B_x|/\mathrm{IMF}|B_t|) \quad (1)$$

Here the "θ" varies from 0° to 90°.

The International Geomagnetic Reference Field model (internal) and the Tsyganenko 96 (T96) model (external) (Tsyganenko & Stern, 1996) were used to trace all FAC cases along the magnetic field lines from the FAC locations in the magnetotail to the polar region. We note that the T96 model uses as input IMF B_y and B_z. Thus, while there is no explicit dependence of the model on the cone angle, the mapping from the tail to the polar region also changes under different IMF conditions. Thus, the mapped invariant latitude depends both on the location where the FAC was observed and on particular parameter inputs to the model for each event. The invariant latitude and the magnetic local time (MLT) were used to show the footprints of the FAC cases.

Figure 1 illustrates an example of the selection of the FAC cases when Cluster crossed the northern PSBL in the magnetotail on 12 September 2001. From top to bottom, the panels are the FAC density (a), magnetic field components (B_x, B_y, and B_z) in geocentric solar magnetospheric (GSM) coordinates measured by Cluster (solid lines) and from the model (dotted lines) (b), plasma $ß$ (c), geomagnetic AE (d), and D_{st} indices (e). The two vertical purple lines indicate the start (09:08 UT) and end (11:36 UT) times of the crossing of the northern PSBL by Cluster. The red stars in panel (a) mark the FAC cases numbered from 1 to 14. Panel (b) shows that both the measured and modeled B_x decreased from about 25 to 15 nT with the same trends during the

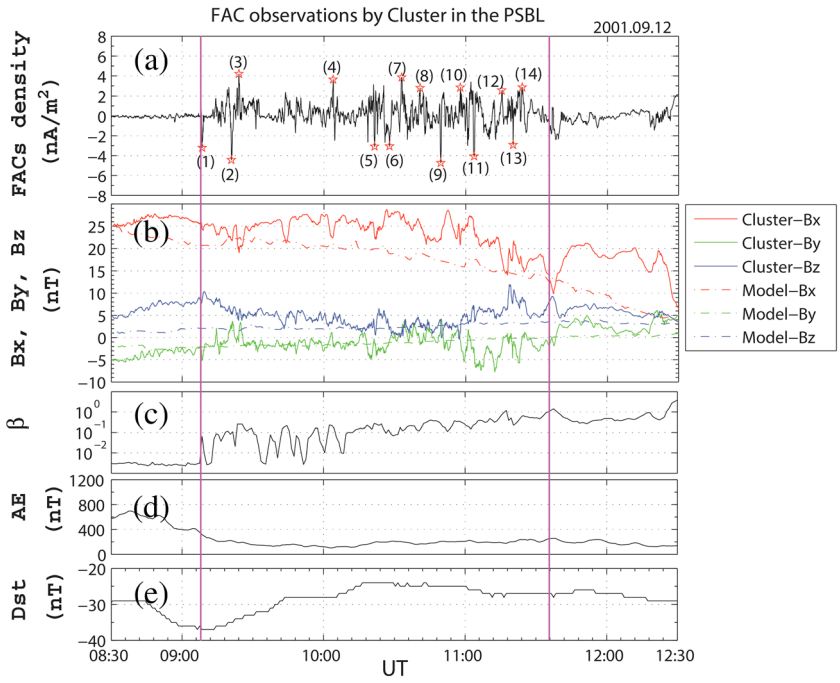

Figure 1. An example of the selection of the field-aligned current (FAC) cases when the Cluster spacecraft were crossing the northern plasma sheet boundary layer (PSBL) in the magnetotail on 12 September 2001. The panels from top to bottom are the FAC density (a), Cluster measured (solid lines) and modeled (dotted lines) magnetic field components B_x, B_y, and B_z (b), plasma ß (c), and AE indices (d) and D_{st} (e). The two vertical purple lines indicate the start (09:08 UT) and end (11:36 UT) times of the crossing. The red stars mark the FAC cases shown with numbers from 1 to 14.

crossing. $B_x > 0$ indicates that the case was taken in the Northern Hemisphere. The fact that the plasma ß increased from about 0.01 to 1 (panel (c)) indicates that Cluster crossed the northern PSBL in the direction from the lobe to the PS region. During the crossing, the value of AE was relatively small (less than 400 nT, panel (d)). The minimum value of D_{st} was only about −37 nT, which shows that the crossing took place in the recovery phase of a small storm (panel (e)). In cases 1 to 14, each footprint in the polar region also depended on the spacecraft position in the PSBL. However, in this paper, which covers 117 Cluster crossings of the PSBL, we just studied the inner and outer boundaries which are controlled by the IMF cone angle.

According to the selection criteria mentioned above, there were 880 FAC cases in the northern PSBL during Cluster crossings from July 2001 to October 2004. We have set limits of 22:00 < MLT < 02:00 to choose the FAC events around local midnight. With this restriction, 542 FAC cases remained.

As to the method of this study, we first calculated the FAC and determined its position in the northern PSBL in the magnetotail. Thereafter, we mapped the position along the field line to the polar region at altitude of 100 km and studied the IMF cone angle influence on the footprints.

3. Statistical Results

3.1. Distribution of the FAC Cases and Their Footprints

Figure 2a provides a schematic illustration showing how the FACs in the magnetotail map to the polar region. The FACs flow from the magnetotail into the polar ionosphere along the magnetic field lines, and the outer (inner) boundary in the magnetotail connects with the poleward (equatorward) boundary in the polar ionosphere.

Figure 2b indicates the locations of the FAC cases in the magnetotail in the *X-Y* plane in the GSM system and the distribution of the footprints in the northern polar region. The red points denote the earthward FAC cases, and the blue points denote the tailward FAC cases. The left two panels show the 542 FAC cases in 2001 (top) and 2004 (bottom), respectively. The lines show the Cluster orbits. The green lines denote that the Cluster data are available, and the yellow lines denote that the Cluster data are not available. The right two panels show the mapping footprints of the FACs in the polar ionosphere in 2001 and 2004, respectively.

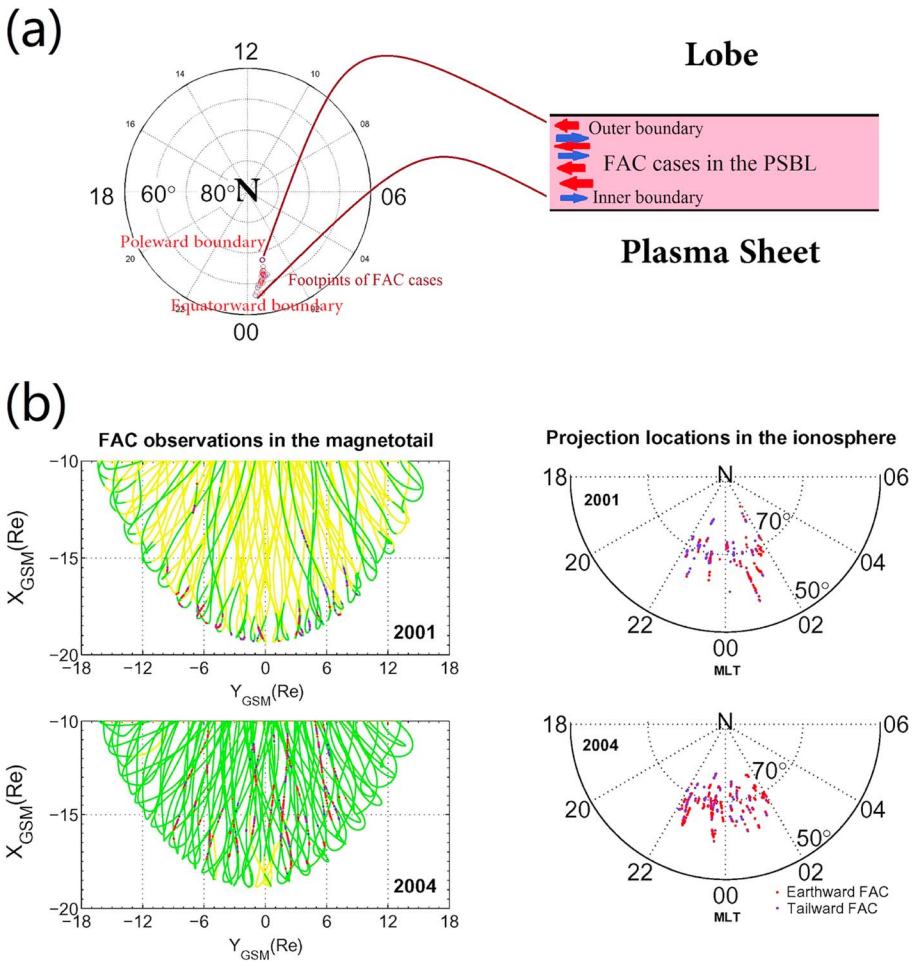

Figure 2. (a) A schematic to show how the field-aligned current (FAC) location in the magnetotail maps into the polar region. (b) The locations of FAC cases in the geocentric solar magnetospheric (GSM) *X-Y* plane (left column) and the footprints in the polar region (right column) in 2001 and 2004; the red color denotes the earthward, and the blue color denotes the tailward ones. The lines show the Cluster orbits, whereby the green color denotes that data are available and the yellow color indicates that the data are not available.

From Figure 2b, we can see that the footprints of the FACs are distributed mainly from 60° to 75° invariant latitude (ILAT), and from 22:00 to 02:00 MLT which corresponds to FAC positions from about $Y_{GSM} = -10$ to 8 R_E in the magnetotail in the Northern Hemisphere. We found that the ILAT of the FAC footprints is related to the IMF cone angle as described in the following section.

3.2. Relationship Between FAC Footprints and IMF Cone Angle

Figure 3 shows the scatter plot of the FAC footprint (ILAT) as a function of the IMF cone angle. Each circle corresponds to an individual FAC case, and the area of the circle represents its density. The red circles denote the large FAC cases with density > 10 nA/m^2. The shaded area shows the IMF cone angle range in which the large FAC cases often occurred.

From Figure 3, we can see that there are almost no FAC cases when the IMF cone angle is less than 10°. With the IMF cone angle increasing, the density of the FACs also increased. This is consistent with the result obtained by Cheng et al. (2013). The large FAC cases occur at lower ILATs (below 71°), and they mainly occur when $\theta > 60°$. There are 35 large FAC cases in total, and 33 of them occur when $\theta > 60°$. The maximum FAC density is 20 nA/m^2 about 1 order of magnitude higher than 2.38 nA/m^2, and it occurs when $\theta = 84°$ at 56° ILAT. This indicates that an increasing IMF cone angle can enhance the disturbance of FAC densities in the magnetotail, and the FAC cases with large densities occur more often under large IMF cone angles.

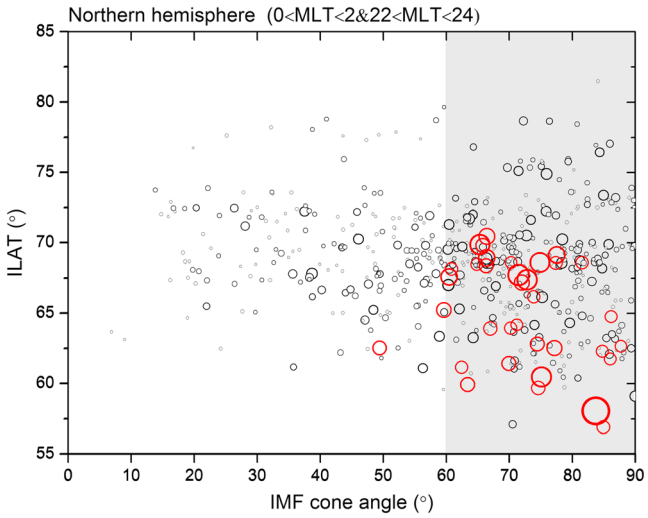

Figure 3. The scatter plot of the FAC footprint (invariant latitude, ILAT) as a function of the interplanetary magnetic field (IMF) cone angle. The circle location indicates the footprint and the area of the circle represents the density of FAC. The red color denotes the large FAC cases with density > 10 nA/m^2. The shaded area shows the IMF cone angle range in which the large field-aligned current cases often occurred. MLT = magnetic local time.

More importantly, from Figure 3 we can see that the ILAT of the equatorward boundary (the bottom edge of the FAC footprints) decreases with increasing IMF cone angle. However, the ILAT of the poleward boundary (the top edge of the FAC footprints) does not change visibly.

In order to investigate the relationship between footprint boundary and IMF cone angle, we used plasma beta to identify the footprints of the FACs in different regions of the PSBL in the magnetotail. Under the condition $0.01 \leq \beta < 0.03$, that is, the FAC is in the outer boundary layer of the PSBL, its polar footprint should be in the poleward boundary layer. If the FAC location lies within $0.7 < \beta \leq 1$, that is, the FAC is in the inner boundary layer of the PSBL, its polar footprint should be in the equatorward boundary layer. Finally, if $0.03 \leq \beta \leq 0.7$, that is, the FAC is in the middle of the PSBL, its polar footprint should be in the middle. As shown in Figure 4, the blue circles indicate the poleward boundary layer of the footprints, and the red circles indicate the equatorward one. This was the basis for studying the influence of the cone angle on the FAC footprints boundary.

The blue (red) line in Figure 4 is the result of a linear fitting for the poleward (equatorward) boundary. The best fit equation is $y = 0.024x + 73.67$, the correlation coefficient R is 0.19, and the P value is 0.1. With this slope, the poleward boundary moves poleward by 0.24° ILAT with every 10° increase of the IMF cone angle. The small R indicates the almost complete absence of correlation between the IMF cone angle and the poleward boundary. For the equatorward boundary, the fitting equation is $y = -0.074x + 66.18$, with $R = 0.72$, and a P value of 0.01. The slope of -0.074 means an equatorward movement of the equatorward boundary by 0.74° ILAT with every 10° increase of the IMF cone angle. There is a close correlation between the IMF cone angle and the equatorward boundary.

As the magnetospheric response is evidently different for southward and northward IMF, we also performed statistics for southward and northward IMF, respectively. In Figure 5, the left panel is for northward IMF (IMF $B_z > 0$) and the right one for southward IMF (IMF $B_z < 0$). The processing steps are the same as for Figure 4. From Figure 5, we can clearly see that there is almost no correlation between the IMF cone angle and the poleward boundary for both northward and southward IMF. However, for the equatorward boundary and northward IMF there is a strong correlation ($R = 0.88$) with the IMF cone angle. For southward IMF, the correlation coefficient between IMF cone angle and the equatorward boundary becomes small ($R = 0.57$).

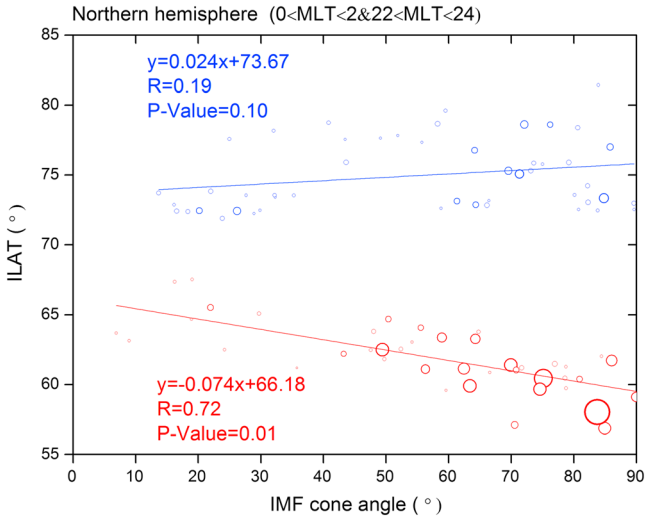

Figure 4. The boundary layers of the footprints of the field-aligned currents in the magnetotail in the invariant latitude (ILAT)-interplanetary magnetic field (IMF) cone angle plane. The blue color indicates the footprint of the field-aligned current in the outer boundary layer ($0.01 \leq \beta < 0.03$), and the red color indicates the one in the inner boundary layer ($0.7 < \beta \leq 1$) of the plasma sheet boundary layer. The lines are the linear fitting results. Only the equatorward boundary has a good correlation with IMF cone angle. MLT = magnetic local time.

From Figure 5, we can see that there is a pronounced gap between the main population of footprints (around 72° ILAT) and the most poleward footprints (around 78° ILAT) for northward IMF only. Iijima et al. (1984) studied the FAC in the dayside auroral region at low altitude and found that when the northward IMF B_z is strong enough, a new FAC called NBZ (Northward IMF Bz) current can form outside the poleward boundary of the Region 1 FAC. A subsequent study found that the NBZ FAC was present not only in the dayside auroral region but also on the nightside and with a complex structure (Iijima & Shibaji, 1987). Our result indicates that the gap in Figure 5 is associated with the NBZ FAC at low altitude. This needs to be studied further. On both sides of the gap, both the main population of footprints and the most poleward footprints respectively have been used to obtain linear fits. The results showed that there is no correlation with IMF cone angle in both cases.

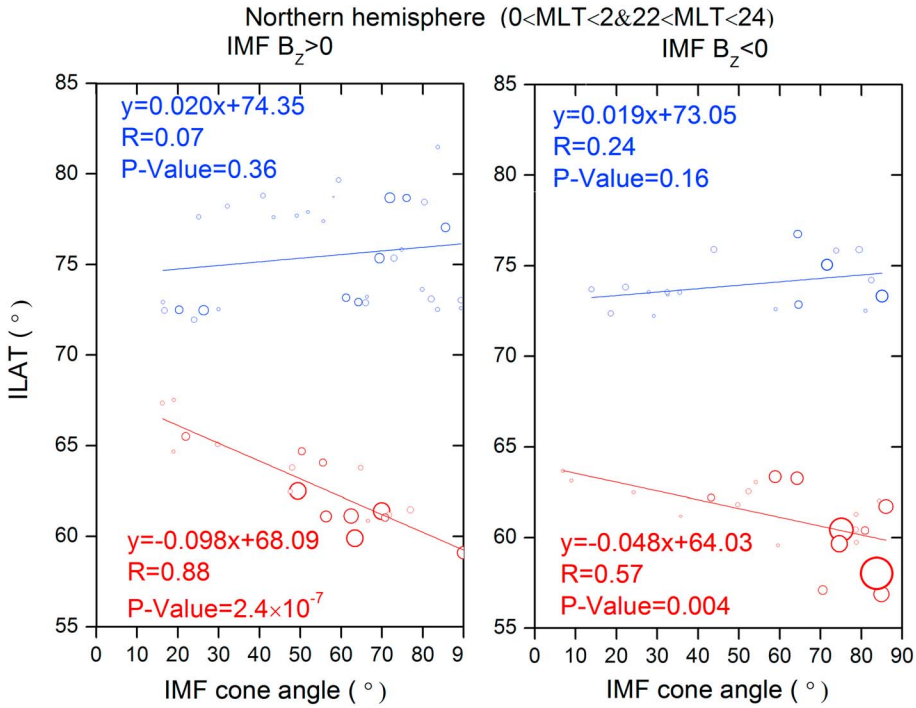

Figure 5. Same as Figure 4 but for different interplanetary magnetic field (IMF) orientations. The poleward boundaries show almost no correlation with IMF cone angle for both northward and southward IMFs. The equatorward boundary has a close correlation with IMF cone angle for southward IMF and a strong correlation with IMF cone angle for northward IMF. ILAT = invariant latitude; MLT = magnetic local time.

Figure 5 shows the boundaries together with the fitting lines. There is a strong negative correlation between the equatorward boundary and IMF cone angle, while there is almost no correlation between the poleward boundary and IMF cone angle. In this research, we have also analyzed the other factors possibly affecting the footprints, such as effects of IMF B_y and B_z. The results show that the IMF cone angle is the dominant influence.

4. Discussion

The magnetic field plays a controlling role in the physical processes in the magnetosphere. Thus, researchers generally use the mapping along the magnetic field lines to study connected phenomena in different magnetospheric regions. (Antonova et al., 2006; Lu et al., 1997; Østgaard et al., 2005; Shevchenko et al., 2010; Trattner et al., 2005; Trattner et al., 2012). Magnetic field lines are also important for the magnetosphere-ionosphere coupling. In order to study the FACs in the magnetotail and its footprints in the polar region, the Tsyganenko 96 (T96) model was used to perform the mapping along the magnetic field lines.

Table 1
The Magnetic Field Component B_x of T96 Model in Comparison With Cluster Observations

Case	B_{xC} (nT)	B_{xM} (nT)	Relative Error (%)
1	23.03	20.65	10.32
2	22.19	22.31	0.53
3	20.39	22.08	8.29
4	22.84	21.28	6.85
5	23.74	20.05	15.54
6	23.08	20.50	11.21
7	25.55	18.31	28.33
8	26.19	18.78	28.26
9	22.10	17.25	21.96
10	22.87	16.06	29.77
11	24.85	17.50	29.57
12	16.41	15.26	6.99
13	16.58	14.49	12.61
14	16.16	14.04	13.12

Note. B_{xC} denotes the B_x of Cluster observations. B_{xM} denotes the B_x of the modeling results.

The T96 model can be used to study different process of space physics (Fenrich et al., 2001; Ni et al., 2011; Zhou et al., 1999). We have made a comparison of the magnetic field component B_x between the Cluster observations and the modeling results (with the International Geomagnetic Reference Field and T96). Table 1 shows the B_x (B_{xC}) observed by Cluster and the one from the model B_x (B_{xM}), and the relative errors of the model to the observation (i.e., $\left|\frac{B_{xC}-B_{xM}}{B_{xC}}\right|\times 100\%$) for the 14 FAC cases in panel (a). The relative errors are less than 30% (maximum is 29.77%, minimum is 0.53%, and the mean value is 15.95%). In this study, we also analyzed the relative errors for all selected FAC cases, and the mean value of

the relative errors was 19.58%, which showed the T96 model was well consistent with the observation during the FAC cases.

The simulation is also a way to study connected phenomena in different magnetospheric regions. Some recent MHD simulations indicate that current lines and field lines sometimes deviate significantly because of the finite diamagnetic currents flowing perpendicular to the magnetic field (Ebihara & Tanaka, 2015; Watanabe et al., 2014). In this paper, we only studied the FAC footprints in the polar region.

Our results show that there is almost no FACs when the IMF cone angle is less than 10°. This indicates that the FAC is weak in the PSBL under the radial IMF condition. H. Wang et al. (2014) reported that, in the nightside ionosphere, the intensity of FACs becomes quite weak in the Northern Hemisphere during the radial IMF period. Their study and ours showed that the same FAC changes existed in the nightside ionosphere and magnetotail under the radial IMF condition, and there might be a connection.

Our result shows that the large FAC cases (density $>$ 10 nA/m^2) occur at low ILATs (below 71°) and mainly occur when the IMF cone angle $\theta > 60°$. It indicates that the footprints of the large FACs mainly extend equatorward when $\theta > 60°$. Our result is consistent with previous work (Ohtani et al., 1988; H. Wang, Lhür, et al., 2006). In this condition, the IMFs B_y and B_z are much bigger than the IMF B_x component and can result in strong disturbances of the geomagnetic field in the magnetotail. Then there will be a higher chance to detect the large FACs at lower ILATs.

Our results show the equatorward boundary of the FAC footprints in the polar region decreases with increasing IMF cone angle. This means if the IMFs B_y and B_z are gradually increasing (relative to the IMF B_x), they can gradually result in stronger and stronger disturbances of the geomagnetic field both in the magnetotail and the polar region. Therefore, the equatorward boundary of the footprints decreases with the IMF cone angle. For the poleward boundary, there is almost no correlation with IMF cone angle. This can be understood such that its movement is limited by an enhanced lobe magnetic flux. A previous study has suggested that the boundaries of the FACs in the polar region are associated with auroral oval boundaries. Xiong et al. (2014) used the FACs in the polar region to determine the auroral oval boundaries. They found that the equatorward boundary of the auroral oval spreads equatorward everywhere (in MLT), while the poleward boundary shows no dependence on geomagnetic activity around midnight. In this study, the boundaries of the footprints of the FACs in the magnetotail seemed consistent with a variation of the boundaries of the auroral oval. The IMF cone angle can control the efficiency of magnetic reconnection both at the magnetopause and in the magnetotail (Cheng et al., 2013; Scurry et al., 1994; Y. Wang, Elphic, et al., 2006). The observed dependence of geomagnetic activity on the orientation of the IMF is expected as a consequence of magnetic reconnection. From the above, we can understand how the IMF cone angle controls the FAC footprints in the polar region.

Our results also show that the equatorward boundary of the FAC footprints in the polar region and IMF cone angle have a bigger correlation coefficient when IMF B_z is northward. We checked the data and found the footprints of FACs could reach lower ILATs and the FAC densities grew large especially during geomagnetic storms or substorms under IMF is southward. When IMF B_z is southward, the reconnection in the magnetopause and magnetotail is most efficient, and the magnetospheric configuration is converted from the nearly closed one into an open one. Maybe it can be understood that the geomagnetic disturbance is strong and continuous, which can influence not only the FAC density but also its projection location, and the footprints can reach lower ILATs while the range of the disturbance increases. However, it needs to be further studied. In fact, for southward IMF B_z, the geomagnetic disturbances can become strong; thus, the correlation coefficient between IMF cone angle and the equatorward boundary becomes small.

In the initial study, we also wanted to study the FACs in the two PSBLs and the asymmetry between north and south. But the FAC cases in the southern PSBL were insufficient, it was mainly because Cluster did not observe FAC cases in inner and outer PSBL (outer boundary $0.01 < \beta < 0.03$ and the inner boundary as $0.7 < \beta < 1$) every crossing, especially in Southern Hemisphere. And there were no inner or outer PSBL FAC cases in some IMF cone angel bin in the Southern Hemisphere. So we could not get enough boundary data to do the same analysis. And the projection locations of the FACs are different for southern PSBL and northern PSBL. So we did not mix the southern data and only studied the FACs in the northern PSBL. If adding Southern Hemisphere measurements, the study could be used to exclude seasonal effects, such as the fact that when one hemisphere was in darkness the other was illuminated. At present the lack of

the data is a major obstacle to the further study of magnetotail FACs, although four Cluster spacecraft can detect more FACs cases in the magnetotail than previous satellites (such as ISEE1/2 and Geotail). In this study, we could only use the existing data to study the FACs in the northern PSBL. We believe this study might lay a foundation for further research.

5. Summary

In this study, we used Cluster spacecraft data to study the influence of the IMF cone angle on the footprints of the observed FACs in the northern PSBL in the magnetotail. The FAC was calculated by the "curlometer" method, and 542 FAC cases have been selected for the present study. We obtained the distribution of the FAC cases in the magnetotail. Thereafter, the T96 model was used to trace the FAC cases along the magnetic field lines to the polar region, and their footprint distribution was obtained.

Our results show that (1) there is almost no FACs when the IMF cone angle is less than 10°, which indicates that the FAC is weak in the PSBLs under the radial IMF condition. (2) The large FAC cases (density $>$ 10 nA/m^2) occur at low ILATs (no more than 71°) and mainly occur when the IMF cone angle $\theta > 60°$. This implies that strong IMFs B_y and B_z (relative to the IMF B_x) can result in a strong disturbance of the geomagnetic field in the magnetosphere, both in the magnetotail and the polar region. (3) The equatorward boundary of the FAC footprints in the polar region decreases with the IMF cone angle for both northward and southward IMF B_z, while there is almost no change of the poleward boundary with IMF cone angle. This shows that the IMF cone angle plays an important controlling role in FAC distributions in the magnetosphere-ionosphere coupling system. The equatorward boundary of the FAC footprints is more responsive to IMF cone angle. This is due to the magnetospheric structure and the response of magnetic field disturbances to the solar wind and IMF. The poleward boundary movement is limited by an enhanced lobe magnetic flux; thus, the poleward boundary of the footprints remains almost unchanged with IMF cone angle.

These results are important for understanding the solar wind-magnetosphere-ionosphere coupling. However, the multiple control mechanisms which might be involved in the process of the boundaries change and need to be studied further.

Acknowledgments
This work was supported by National Natural Science Foundation of China under grants 41474137, 41674145, and 41374169, and the Specialized Research Fund for State Key Laboratories. IMF data, AE, and D_{st} were obtained from the GSFC/SPDF OMNIWeb interface at http://omniweb.gsfc.nasa.gov. The authors thank the Cluster team for their data and software. Z. W. Cheng also thanks C. G. Mouikis and E. Lund for their help and discussion.

References

Antonova, E. E., Kirpichev, I. P., & Stepanova, M. V. (2006). Field-aligned current mapping and the problem of the generation of magnetospheric convection. *Advances in Space Research*, *38*(8), 1637–1641. https://doi.org/10.1016/j.asr.2005.09.042

Balogh, A., Carr, C. M., Acuña, M. H., Dunlop, M. W., Beek, T. J., Brown, P., et al. (1997). The Cluster magnetic field investigation. *Space Science Reviews*, *19*(10/12), 1207–1217. https://doi.org/10.5194/angeo-19-1207-2001

Cheng, Z. W., Shi, J. K., Dunlop, M., & Liu, Z. X. (2013). Influences of the interplanetary magnetic field clock angle and cone angle on the field-aligned currents in the magnetotail. *Geophysical Research Letters*, *40*, 5355–5359. https://doi.org/10.1002/2013GL056737

Choy, L. W., Arnoldy, R. L., Potter, W., Kintner, P., & Cahill, L. J. Jr. (1971). Field-aligned particle currents near an auroral arc. *Journal of Geophysical Research*, *76*(34), 8279–8298. https://doi.org/10.1029/JA076i034p08279

Cummings, W. D., & Dessler, A. J. (1967). Field-aligned currents in the magnetosphere. *Journal of Geophysical Research*, *72*(3), 1007–1013. https://doi.org/10.1029/JZ072i003p01007

Dunlop, M. W., Southwood, D. J., Glassmeier, K. -H., & Neubauer, F. M. (1988). Analysis of multipoint magnetometer data. *Advances in Space Research*, *8*(9-10), 273–277. https://doi.org/10.1016/0273-1177(88)90141-X

Dušík, Š., Granko, G., Šafránková, J., Němeček, Z., & Jelínek, K. (2010). IMF cone angle control of the magnetopause location: Statistical study. *Geophysical Research Letters*, *37*, L19103. https://doi.org/10.1029/2010GL044965

Ebihara, Y., & Tanaka, T. (2015). Substorm simulation: Formation of westward traveling surge. *Journal of Geophysical Research: Space Physics*, *120*, 10,466–10,484. https://doi.org/10.1002/2015JA021697

Elphic, R. C., Bonnell, J. W., Strangeway, R. J., Kepko, L., Ergun, R. E., McFadden, J. P., et al. (1998). The auroral current circuit and field-aligned currents observed by FAST. *Geophysical Research Letters*, *25*(12), 2033–2036. https://doi.org/10.1029/98GL01158

Fenrich, F. R., Luhmann, J. G., Fedder, J. A., Slinker, S. P., & Russell, C. T. (2001). A global MHD and empirical magnetic field model investigation of the magnetospheric cusp. *Journal of Geophysical Research*, *106*(A9), 18,789–18,802. https://doi.org/10.1029/2001JA900040

Frank, L. A. (1981). Field-aligned currents in Earth's magnetotail. *Journal of Geophysical Research*, *86*(A2), 687–700. https://doi.org/10.1029/JA086iA02p00687

Gjerloev, J. W., Ohtani, S., Iijima, T., Anderson, B., Slavin, J., & Le, G. (2011). Characteristics of the terrestrial field-aligned current system. *Annales de Geophysique*, *29*(10), 1713–1729. https://doi.org/10.5194/angeo-29-1713-2011

Hesse, M., & Birn, J. (1991). On depolarization and its relation to the substorm current wedge. *Journal of Geophysical Research*, *96*(A11), 19417–19,426. https://doi.org/10.1029/91JA01953

Hones, E. W. (1979). Transient phenomena in the magnetotail and their relation to substroms. *Space Science Reviews*, *23*(3), 393–410.

Iijima, T., & Potemra, T. A. (1978). Large-scale characteristics of field-aligned currents associated with substorms. *Journal of Geophysical Research*, *83*(A2), 599–615. https://doi.org/10.1029/JA083iA02p00599

Iijima, T., Potemra, T. A., Zanetti, L. J., & Bythrow, P. F. (1984). Large-scale Birkeland currents in the dayside polar region during strongly northward IMF: A new Birkeland current system. *Journal of Geophysical Research*, *89*(A9), 7441–7452. https://doi.org/10.1029/JA089iA09p07441

Iijima, T., & Shibaji, T. (1987). Global characteristics of northward IMF associated (NBZ) field-aligned currents. *Journal of Geophysical Research*, *92*(A3), 2408–2424. https://doi.org/10.1029/JA092iA03p02408

Johnstone, A. D., Alsop, C., Burge, S., Carter, P. J., Coker, A. J., Fazakerley, A. N., et al. (1997). Peace: A plasma electron and current experiment. *Space Science Reviews*, *79*(1/2), 351–398. https://doi.org/10.1023/A:1004938001388

Juusola, L., Kauristie, K., Amm, O., & Ritter, P. (2009). Statistical dependence of auroral ionospheric currents on solar wind and geomagnetic parameters from 5 years of CHAMP satellite data. *Annales de Geophysique*, *27*(3), 1005–1017. https://doi.org/10.5194/angeo-27-1005-2009

Kavosi, S., & Raeder, J. (2015). Ubiquity of Kelvin–Helmholtz waves at Earth's magnetopause. *Nature Communications*, *6*(1), 7019. https://doi.org/10.1038/ncomms%208019

Li, W., Knipp, D., Lei, J., & Raeder, J. (2011). The relation between dayside local Poynting flux enhancement and cusp reconnection. *Journal of Geophysical Research*, *116*, A08301. https://doi.org/10.1029/2011JA016566

Lu, G., Siscoe, G. L., Richmond, A. D., Pulkkinen, T. I., Tsyganenko, N. A., Singer, H. J., & Emery, B. A. (1997). Mapping of the ionospheric field-aligned currents to the equatorial magnetosphere. *Journal of Geophysical Research*, *102*(A7), 14,467–14,476. https://doi.org/10.1029/97JA00744

Ma, X., & Otto, A. (2013). Mechanisms of field-aligned current formation in magnetic reconnection. *Journal of Geophysical Research: Space Physics*, *118*, 4906–4914. https://doi.org/10.1002/jgra.50457

Masakazu, W., & Sofko, G. J. (2009). Dayside four-sheet field-aligned current system during IMF B_y-dominated periods. *Journal of Geophysical Research*, *114*, A03208. https://doi.org/10.1029/2008JA013815

Morooka, M., Mukai, T., & Fukunishi, H. (2004). Current-voltage relationship in the auroral particle acceleration region. *Annales de Geophysique*, *22*(10), 3641–3655. https://doi.org/10.5194/angeo-22-3641-2004

Ni, B., Thorne, R. M., Shprits, Y. Y., Orlova, K. G., & Meredith, N. P. (2011). Chorus-driven resonant scattering of diffuse auroral electrons in nondipolar magnetic fields. *Journal of Geophysical Research*, *116*, A06225. https://doi.org/10.1029/2011JA016453

Ohtani, S., Kokubun, S., Elphic, R. C., & Russell, C. T. (1988). Field-aligned current signatures in the near-tail region: 1. ISEE observations in the plasma sheet boundary layer. *Journal of Geophysical Research*, *93*(A9), 9709–9720. https://doi.org/10.1029/JA093iA09p09709

Østgaard, N., Tsyganenko, N. A., Mende, S. B., Frey, H. U., Immel, T. J., Fillingim, M., et al. (2005). Observations and model predictions of substorm auroral asymmetries in the conjugate hemispheres. *Geophysical Research Letters*, *32*, L05111. https://doi.org/10.1029/2004GL022166

Pytte, T., McPherron, R. L., & Kokubun, S. (1976). The ground signatures of the expansion phase during multiple onset substorms. *Planetary and Space Science*, *24*(12), 1115–1IN4. https://doi.org/10.1016/0032-0633(76)90149-5

Rème, H., Aoustin, C., Bosqued, J. M., Dandouras, I., Lavraud, B., Sauvaud, J. A., et al. (2001). First multispacecraft ion measurements in and near the Earth's magnetosphere with the identical Cluster ion spectrometry (CIS) experiment. *Annales de Geophysique*, *19*(10/12), 1303–1354. https://doi.org/10.5194/angeo-19-1303-2001

Scholer, M., & Otto, A. (1991). Magnetotail reconnection: Current diversion and field-aligned currents. *Geophysical Research Letters*, *18*(4), 733–736. https://doi.org/10.1029/91GL00361

Scurry, L., Russell, C. T., & Gosling, J. T. (1994). Geomagnetic activity and the beta dependence of dayside reconnection rate. *Journal of Geophysical Research*, *99*(A8), 14,811–14,814. https://doi.org/10.1029/94JA00794

Shevchenko, I. G., Sergeev, V., Kubyshkina, M., Angelopoulos, V., Glassmeier, K. H., & Singer, H. J. (2010). Estimation fo magnetosphere-ionosphere mapping accuracy using isotropy boundary and THEMIS observations. *Journal of Geophysical Research*, *115*, A11206. https://doi.org/10.1029/2010JA015354

Shi, J. K., Cheng, Z. W., Zhang, T. L., Dunlop, M., Liu, Z. X., Torkar, K., et al. (2010). South-north asymmetry of field-aligned currents in the magnetotail observed by Cluster. *Journal of Geophysical Research*, *115*, A07228. https://doi.org/10.1029/2009JA014446

Shi, J. K., Zhang, Z., Torkar, K., Dunlop, M., Fazakerley, A., Cheng, Z., & Liu, Z. (2014). Temporal and spatial scales of a high-flux electron disturbance in the cusp region: Cluster observations. *Journal of Geophysical Research: Space Physics*, *119*, 4536–4543. https://doi.org/10.1002/2013JA019560

Taguchi, S., Sugiura, M., Iyemori, T., Winningham, J. D., & Slavin, J. A. (1992). By-controlled convection and field-aligned currents near midnight auroral oval for northward interplanetary magnetic field. *Journal of Geophysical Research*, *97*(A8), 12,231–16,044. https://doi.org/10.1029/92JA00548

Takahashi, K., McPherron, R. L., & Terasawa, T. (1984). Dependence of the spectrum of Pc 3–4 pulsations on the interplanetary magnetic field. *Journal of Geophysical Research*, *89*, 2770–2780. https://doi.org/10.1029/JA089iA05p02770

Trattner, K. J., Fuselier, S. A., Petrinec, S. M., Yeoman, T. K., Mouikis, C., Kucharek, H., & Reme, H. (2005). Reconnection sites of spatial cusp structures. *Journal of Geophysical Research*, *110*, A04207. https://doi.org/10.1029/2004JA010722

Trattner, K. J., Petrinec, S. M., Fuselier, S. A., Omidi, N., & Sibeck, D. G. (2012). Evidence of multiple reconnection lines at the magnetopause from cusp observations. *Journal of Geophysical Research*, *117*, A01213. https://doi.org/10.1029/2011JA017080

Tsyganenko, N. A., & Stern, D. P. (1996). Modeling the global magnetic field of the large-scale Birkeland current systems. *Journal of Geophysical Research*, *101*(A12), 27,187–27,198. https://doi.org/10.1029/96JA02735

Ueno, G., Ohtani, S., Saito, Y., & Mukai, T. (2002). Field-aligned currents in the outermost plasma sheet boundary layer with Geotail observation. *Journal of Geophysical Research*, *107*(A11), 1399. https://doi.org/10.1029/2002JA009367

Wang, H., Lühr, H., Ma, S. Y., Weygand, J., Skoug, R. M., & Yin, F. (2006). Field-aligned currents observed by CHAMP during the intense 2003 geomagnetic storm events. *Annales de Geophysique*, *24*(1), 311–324. https://doi.org/10.5194/angeo-24-311-2006

Wang, H., Lühr, H., Shue, J.-H., Frey, H. U., Kervalishvili, G., Huang, T., et al. (2014). Strong ionospheric field-aligned currents for radial interplanetary magnetic fields. *Journal of Geophysical Research: Space Physics*, *119*, 3979–3995. https://doi.org/10.1002/2014JA019951

Wang, Y. L., Elphic, R. C., Lavraud, B., Taylor, M. G. G. T., Birn, J., Russell, C. T., et al. (2006). Dependence of flux transfer events on solar wind conditions from 3 years of Cluster observations. *Journal of Geophysical Research*, *111*, A04224. https://doi.org/10.1029/2005JA011342

Watanabe, M., Sakito, S., Tanaka, T., Shinagawa, H., & Murata, K. T. (2014). Global MHD modeling of ionospheric convection and field-aligned currents associated with IMF B_y triggered theta auroras. *Journal of Geophysical Research: Space Physics*, *119*, 6145–6166. https://doi.org/10.1002/2013JA019480

Wild, J. A., Milan, S. E., Owen, C. J., Bosqued, J. M., Lester, M., Wright, D. M., et al. (2004). The location of the open-closed magnetic field line boundary in the dawn sector auroral ionosphere. *Annales de Geophysique*, *22*(10), 3625–3639. https://doi.org/10.5194/angeo-22-3625-2004

Xiong, C., Lühr, H., Wang, H., & Johnsen, M. G. (2014). Determining the boundaries of the auroral oval from CHAMP field-aligned current signatures—Part 1. *Annales de Geophysique*, *32*(6), 609–622. https://doi.org/10.5194/angeo-32-609-2014

Yamauchi, M., & Araki, T. (1989). The interplanetary magnetic field *By*-dependent field-aligned current in the dayside polar cap under quiet conditions. *Journal of Geophysical Research*, *94*(A3), 2684–2690. https://doi.org/10.1029/JA094iA03p02684

Zhou, X. W., Russell, C. T., Le, G., Fuselier, S. A., & Scudder, J. D. (1999). The polar cusp location and its dependence on dipole tile. *Geophysical Research Letters*, *26*(3), 429–432. https://doi.org/10.1029/1998GL900312

Zmuda, A. J., Martin, J. H., & Heuring, F. T. (1966). Transverse magnetic disturbances at 1100 kilometers in the auroral region. *Journal of Geophysical Research*, *71*(21), 5033–5045. https://doi.org/10.1029/JZ071i021p05033